LWT - Food Science and Technology 131 (2020) 109723

Contents lists available at ScienceDirect

LWT - Food Science and Technology

journal homepage: www.elsevier.com/locate/lwt

Inclusion complexation of catechins-rich green tea extract by β-cyclodextrin: Preparation, physicochemical, thermal, and antioxidant properties

Chagam Koteswara Reddy[a], Eun Sung Jung[b,**], Su Young Son[a], Choong Hwan Lee[a,b,c,*]

[a] Department of Bioscience and Biotechnology, Konkuk University, Seoul, 05029, Republic of Korea
[b] Department of Systems Biotechnology, Konkuk University, Seoul, 05029, Republic of Korea
[c] Research Institute for Bioactive-Metabolome Network, Konkuk University, Seoul, 05029, Republic of Korea

ARTICLE INFO

Keywords:
Green tea
β-cyclodextrin
Inclusion complex
UHPLC-LTQ-Orbitrap-MS
FE-SEM

ABSTRACT

Green tea (*Camellia sinensis*) is a traditional beverage. Its ethanolic extract (GTE) is rich in catechins, has a wide range of associated health benefits. However, the commercial formulations of catechins-rich GTE are limited owing to its low thermal stability and high oxidation sensitivity. In this study, an inclusion complexes of GTE-β-cyclodextrin (GTE-β-CD) were prepared by freeze-drying. Structural characteristics of the inclusion complexes were examined using FE-SEM, XRD, FT-IR, and TGA/DTG. After inclusion complexation, the samples were analyzed by UHPLC-LTQ-Orbitrap-MS and the variation in the quantities of each identified metabolite were visualized in the heat map. Results revealed that bioactive components of GTE were successfully included in β-CD cavities and the thermal stability of GTE was increased by complexation with β-CD. Results of UHPLC-LTQ-Orbitrap-MS confirmed that β-CD had selective inclusion capacity for bioactive compounds of green tea. A variety of *in-vitro* antioxidant studies (DPPH, ABTS, and FRAP) revealed that the GTE-β-CD inclusion complexes contained better scavenging capacity against free radicals. Findings of the present work suggest that the GTE-β-CD inclusion complexes might have potential applications as functional ingredient and health supplement.

1. Introduction

Green tea is a traditional beverage produced from the evergreen plant *Camellia sinensis*. It is one of the popular daily consumed beverages worldwide, especially in Asia (Kim et al., 2008). Green tea is rich in polyphenols, caffeine, polysaccharides, and other bioactive components (Ye et al., 2020). Because of its eminent health effects such as antioxidant, anti-diabetic, anti-bacterial, anti-viral, anti-carcinogenic, anti-inflammatory, and hypocholesterolemic activities (Bancirova, 2010; Kim et al., 2008; Lorenzo & Munekata, 2016; Zaveri, 2006), it has been widely used as a health-promoting beverage. The major components of the ethanolic extract of green tea (GTE) are catechins and flavonols that contribute to its antioxidant properties (Jung et al., 2017). In addition, green tea has some other physiological functions such as reducing obesity, managing the gastrointestinal environment, healing wounds, and increasing the density of bone minerals (Kao, Hiipakka, & Liao, 2000; Zaveri, 2006). Due to their biological activities, the use of flavonoids in food and pharmaceutical industries seems to be very attractive. However, the biological activities of flavonoids depend on their chemical structure, thermal stability, degree of hydroxylation and degree of polymerization (Fang & Bhandari, 2010; Liu et al., 2016). Additionally, the applications of flavonoids especially catechins in the food industry is inadequate due to their low thermal stability, poor aqueous solubility, astringent and bitter taste, and sensitivity to oxidation (Fang & Bhandari, 2010; Ho, Thoo, Young, & Siow, 2017). Interestingly, these shortcomings can be overcome by the process of encapsulation.

In recent years, a few research groups have described that inclusion complexes and/or encapsulation of guest molecules can increase the thermal stability and bioactivity of guest materials against thermal processing, light, and storage, increases their aqueous solubility, and mask and/or reduce their undesired tastes (Fang & Bhandari, 2010; Ho et al., 2017; Liu et al., 2016). Cyclodextrins are cyclic oligomers of α-D-glucopyranose made from starch by enzymatic hydrolysis (Zhang et al., 2017). At its molecular level, cyclodextrin molecule contains a lipophilic central cavity and a hydrophilic outer surface with many hydroxyl groups (Cai, Yuan, Cui, Wang, & Yue, 2018). This peculiar feature enables cyclodextrin to act as a host molecule that may produce inclusion complexes with a variety of hydrophobic guest compounds. Among various cyclodextrins, β-cyclodextrin (β-CD) is the most

* Corresponding author. Department of Bioscience and Biotechnology, Konkuk University, Seoul, 05029, Republic of Korea.
** Corresponding author.
E-mail addresses: jes708@konkuk.ac.kr (E.S. Jung), chlee123@konkuk.ac.kr (C.H. Lee).

https://doi.org/10.1016/j.lwt.2020.109723
Received 1 April 2020; Received in revised form 5 May 2020; Accepted 5 June 2020
Available online 16 June 2020

accessible one because of their appropriate cavity size, non-toxicity, biocompatibility, and biodegradability (Del Valle, 2004). Many polyphenols and flavonoids are capable to forming inclusion complexes with β-CD. Furthermore, the inclusion complexation of various guest molecules by β-CD has been widely described in the fields of food science, pharmacology, and cosmetics (Hsu, Yu, Tsai, & Tsai, 2013; Lu, Lee, Mau, & Lin, 2010).

In recent years, some studies have been accomplished to expand the stability and solubility of inclusion complexes of polyphenols with β-CD. Krishnaswamy, Orsat, and Thangavel (2012) have described that the inclusion complexation of catechin with β-CD by co-precipitation can strengthen the stability and controlled release pattern of catechin. Wang, Cao, Sun, and Wang (2011) have prepared an inclusion complexes of polyphenols with β-CD by freeze-drying to improve the stability and aqueous solubility of the polyphenols. Further, Han, Zhang, Shen, Zheng, & Zhang, 2019 have reported that the complex formation between ferulic acid and β-CD can enhance the thermal stability, photostability, and solubility of ferulic acid. Recently, instead of using a single bioactive compound as a guest material, crude extract of plants including garlic oil, olive leaf, grape seed, cinnamon oil, and medical herbs (Chen, Chen, Guo, Li, & Li, 2007; Fang & Bhandari, 2010; Jaski et al., 2019; Wen et al., 2016) that contain multiple compounds have been complexed with host materials to form inclusion complexes to expand the solubility, thermal stability, functional and biological activities of these compounds.

However, to the best of our knowledge, inclusion complexation of ethanolic extract of green tea (GTE) with β-CD and its metabolite profile, thermal analysis, physicochemical and antioxidant properties have not been reported yet. Thus, the objective of this work was to prepare an inclusion complexes of catechins-rich GTE with β-CD by freeze-drying. Structural characteristics of GTE-β-CD inclusion complexes were analyzed by field-emission scanning electron microscopy, X-ray diffractometry, thermogravimetry/derivative thermogravimetry, and Fourier-transform infrared spectroscopy. After inclusion complexation, the metabolites of GTE were examined by ultra-high-performance liquid chromatography-linear trap quadrupole-orbitrap-tandem mass spectrometry (UHPLC-LTQ-Orbitrap-MS) and difference in content of each identified bioactive compound was determined. Also, the antioxidant activity of inclusion complex was evaluated by measuring the clearance of DPPH and $ABTS^{+}$ radicals.

2. Materials and methods

2.1. Materials

The dried and powdered form of ethanolic extract of green tea (GTE) was supplied by AmorePacifc Co. (Seoul, Korea). It contained 27.58% of catechins, including epigallocatechin gallate (13.28%), epigallocatechin (7.50%), epicatechin gallate (4.24%), and epicatechin (2.56%). β-Cyclodextrin (β-CD), epicatechin, epigallocatechin gallate, epigallocatechin, epicatechin gallate, 2,2-diphenyl-1-picrylhydrazyl (DPPH), and 2,21-azinobis(3-ethylbenzothiazoline-6-sulfonic acid) diammonium salt (ABTS) were purchased from Sigma-Aldrich Co. (St. Louis, MO, USA) and used as-received. Other reagents and chemicals were of analytical grade.

2.2. Preparation of GTE-β-CD inclusion complexes

The GTE-β-CD inclusion complexes between catechins-rich green tea extract (GTE) and β-cyclodextrin (β-CD) were prepared, following a procedure described by Zhang et al. (2017) and Aree and Jongrungruangchok (2016) with minor modifications. To prepare GTE-β-CD inclusion complexes, first, β-CD (400 mg, dry basis) was suspended in 40 mL of deionized water by stirring at 60 °C for 20 min in a water bath. Afterward, 5 mL of pre-dissolved GTE (50 mg or 100 mg, dry basis) in absolute ethanol was slowly added into the β-CD aqueous dispersion. Then the solution was continuously stirred at 60 °C in the dark for 5 h in a water bath to permit greater interaction between β-CD and GTE to form an inclusion complex. After incubation, the solution was filtered through a 0.45 μm filter to eliminate insoluble particles. The soluble filtrate was then frozen at −80 °C and subsequently freeze-dried using a lyophilizer for 48 h to achieve the inclusion complex. Finally, the resulted GTE-β-CD inclusion complex powder was stored in an airtight bottle at 4 °C for further use.

2.3. Preparation of GTE-β-CD physical mixture

To prepare a physical mixture of GTE-β-CD, accurately weighed β-CD (400 mg) and GTE (50 or 100 mg) was ground in a mortar until the blend was homogeneous. The resulted physical mixture was stored in an airtight bottle at 4 °C for further use.

2.4. Measurements and characterization

Morphology of the samples were analyzed by field-emission scanning electron microscopy (FE-SEM, Hitachi S-4800, Tokyo, Japan). Prior to analysis, samples were fixed on an aluminum stub with adhesive tape and vacuum coated with a fine layer of palladium to improve conductivity. X-ray diffractometer (XRD; Philips XPERT MPD, Almelo, Netherlands) was used to study the crystalline structures of the samples. Data were scientifically collected from 3° to 30° (2θ) with a scanning rate of 1.5°/min. Fourier transform infrared spectrometer (FTIR, Bruker, Germany) was used to record the infrared spectra (4000–500 cm^{-1}; 64 scans; 4 cm^{-1} resolution) of the samples. Thermal stability of the samples were measured by thermo-gravimetric analyzer (TGA, TA Q500, New Castle, USA). TGA analysis were carried out under nitrogen atmosphere from 30 to 900 °C at a heating rate of 10 °C/min.

2.5. UHPLC-LTQ-orbitrap-MS analysis

For metabolite extraction, 10 mg of each sample was dissolved in 20 mL of methanol, shaken for 60 min, and then ultra-sonicated for 15 min. Then, the suspension was filtered through a 0.2-μm filter, vacuum dried, and stored at −20 °C. Prior to analysis, each sample extract (10 mg/mL) was dissolved in methanol, filtered, and then shifted to an LC vial.

The metabolite profiles of each sample extract were analyzed by ultra-high-performance liquid chromatography-linear trap quadrupole-orbitrap-tandem mass spectrometry (UHPLC-LTQ-Orbitrap-MS). UHPLC system was paired with a binary pump (Thermo Fisher Scientific), an autosampler, and a detector. The chromatographic separation for each sample extract was done on a Phenomenex KINETEX® C18 column (100 mm × 2.1 mm, 1.7 μm) using a mobile phase consist of formic acid (0.1%) in water (solvent A) and in acetonitrile (solvent B). The linear gradient elution designed as follows: 0–1 min, 5% B; 1–10 min, 5–100% B, 10–11 min, 100% B, 11–14 min, 100-5% B. The flow rate, injection volume, and column temperature were set to 0.3 mL/min, 5 μL, and 40 °C, respectively. Mass spectra was recorded by full-spectrum mode covering 100–1000 m/z using an Orbitrap Velos Pro™ system consist of an ion trap mass spectrometer (Thermo Fisher Scientific) paired with a HESI-II probe. Mass spectrometry detections was designed as follows: capillary temperature, 350 °C; probe heater, 300 °C; and capillary voltage, 2.5 kV in negative mode and 3.7 kV in positive mode. Discriminant metabolites were tentatively identified by comparing their molecular weight, mass fragment patterns, and retention time with those of standard compounds using as in-house library data and references.

2.6. Data processing and multivariate statistical analysis

The software Xcalibur (version 2.1) was used for transforming the raw data derived from UHPLC-LTQ-Orbitrap-MS into netCDF. After

conversion, the software MetAlign (http://www.metalign.nl) was used for preprocessing of netCDF data to acquire peak extraction, retention time correction, peak intensity normalization, and accurate masses. Subsequent data were transferred to an Excel sheet and Multivariate statistical analysis was executed by SIMCA-P+ (version 12.0). To compare discriminated metabolites among experimental groups, PCA and PLS-DA were performed.

2.7. Antioxidant activity analysis of GTE-β-CD inclusion complexes

DPPH, ABTS, and FRAP radical scavenging assays were employed to measure antioxidant activities of GTE-β-CD inclusion complexes which were dissolved in methanol (5 mg/10 mL), shaken, and ultra-sonicated until totally homogeneous and filtered. The filtrate was used for the antioxidant activity determination. Antioxidant activity assays such as DPPH, ABTS, and FRAP were performed, following a previous method reported by Jung et al. (2017).

2.8. Statistical analysis

All results were shown as means with standard deviations of triplicate analysis. Statistical significance ($p < 0.05$) between treatments was performed by one-way ANOVA followed by Duncan's test using SPSS software (version 22.0, IBM, Chicago, IL, USA).

3. Results and discussion

3.1. FE-SEM analysis

FE-SEM was employed to qualitatively assess the morphological features of raw materials and their inclusion complexes. Fig. 1 shows the FE-SEM photographs of GTE, β-CD, and their GTE-β-CD inclusion complexes (GTCD-IC50 and GTCD-IC100) and physical mixtures (GTCD-PM50 and GTCD-PM100). These results revealed that the GTE existed in amorphous broken spherical particles as dispersed entities (Fig. 1a), whereas β-CD appeared in crystalline state with different sizes of irregular rectangularly shaped blocky particles (Fig. 1b). Also, there were small particles sticking to the surfaces of large crystals. As can be seen from the FE-SEM photographs, the physical mixtures showed the combination of GTE and β-CD structure, while GTE particles adhered to the β-CD surface (Fig. 1c–d). However, no structural difference in particle size or shape was observed between the physical mixture and β-CD, indicating that no inclusion complex was formed in the physical mixtures. Again, the GTE-β-CD inclusion complexes (Fig. 1e–f) showed irregular particles in which the unique morphology of host and guest molecules disappeared while compact and plate-like structure with crystal particles were observed (Pu et al., 2018). The assessment of these photographs disclosed that the inclusion complex was structurally different from the host and guest materials, and their physical mixtures (Devasari et al., 2015). All these phenomena suggest that morphological features of the GTE-β-CD inclusion complex are entirely dissimilar from those of GTE and β-CD molecules, thus confirming the successful preparation of the GTE-β-CD inclusion complexes.

3.2. XRD analysis

X-ray diffractometry (XRD) is an effective technique for studying the inclusion complexes in powder or microcrystalline state. After complex formation, the diffraction pattern of inclusion complexes is unique from that of the superimposition of host and guest constituents. XRD profiles of the β-CD, GTE, GTE-β-CD inclusion complexes, and physical mixtures are illustrated in Fig. 2. The crystalline structures of β-CD and its inclusion complexes are categorized mostly into three types: channel-type, cage-type, and layer-type (Okumura, Kawaguchi, & Harada, 2003). As shown in Fig. 2, the XRD pattern of GTE showed a large broad peak (2θ), indicating that GTE primarily existed in an amorphous state. XRD profile of β-CD showed intense and sharp peaks (2θ) at 4.48°, 9.04°, 10.71°, 12.55°, 13.52°, 18.01°, 18.92°, 22.71°, and 27.16° with several minor peaks (2θ) at 14.74°, 15.42°, 21.14°, and 25.73°, confirming that β-CD exhibits a typical cage-type structure.

XRD profiles of physical mixtures showed some typical peaks attributable to crystalline and cage-type structure of β-CD with a partial change in peak intensity, suggesting that no new crystal was formed. In contrast, XRD profiles of GTE-β-CD inclusion complexes showed the desertion of peaks (2θ) at 4.48° and 9.04° previously belonged to β-CD molecule. Subsequently, some new sharp peaks (2θ) at 10.71°, 12.53°,

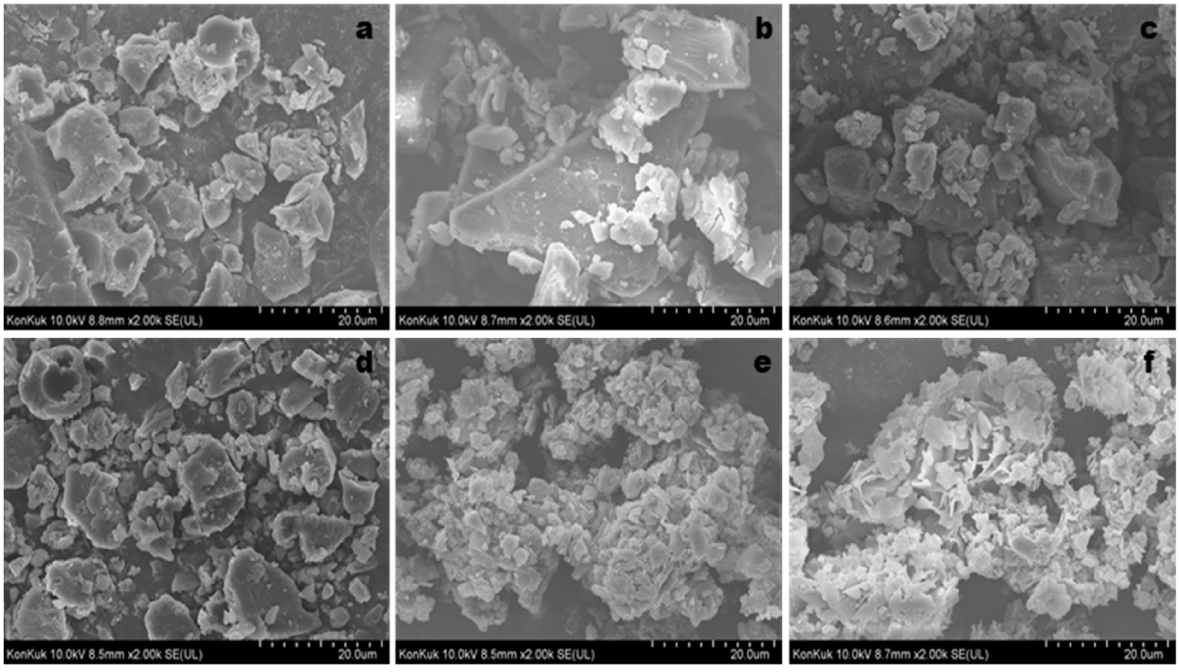

Fig. 1. FE-SEM photographs of ethanolic extract of green tea (**a**), β-cyclodextrin (**b**), physical mixtures (**c** and **d**), and inclusion complexes (**e** and **f**) at 2000 × magnification.

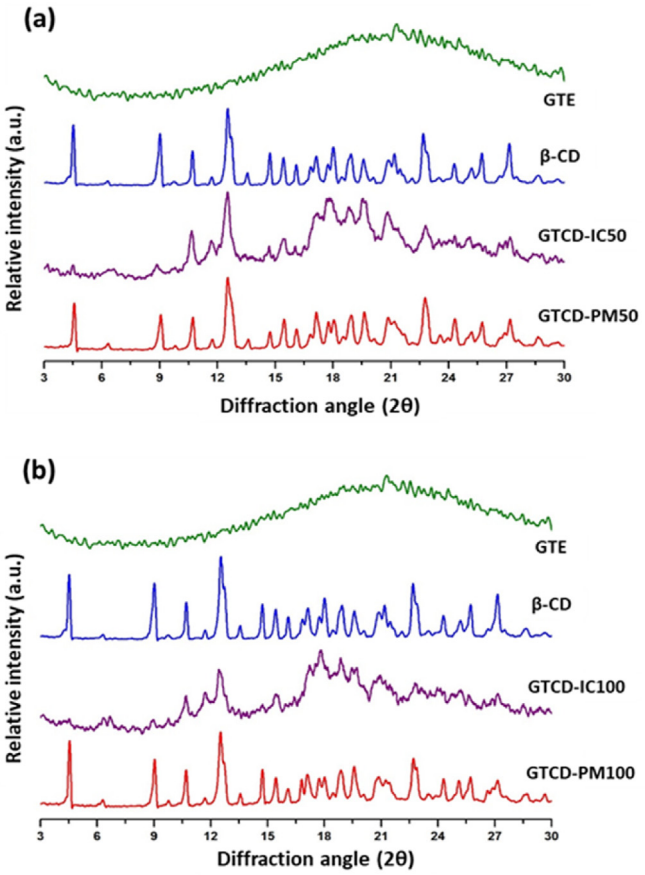

Fig. 2. XRD patterns of ethanolic extract of green tea (GTE), β-cyclodextrin (β-CD), physical mixtures (GTCD-PM50 and GTCD-PM100), and inclusion complexes (GTCD-IC50 and GTCD-IC100). (For interpretation of the references to colour in this figure legend, the reader is referred to the Web version of this article.)

17.80°, 18.86°, 20.89°, and 22.81° were observed in the XRD profile of the inclusion complexes. The appearance of new peaks could be due to alterations in the molecular structure of the β-CD's from cage-type to channel-type packing, confirming the complexation of GTE-β-CD (Okumura et al., 2003; Zhang et al., 2017). Moreover, the freeze-dried inclusion complex exhibited a relatively lower degree of crystallinity with new solid crystalline peaks in the XRD profile.

3.3. FT-IR analysis

FT-IR analysis was used to identify and confirm the complex formation through vibrational deviations upon interactions among host and guest molecules. The spectrums of the β-CD, GTE, GTE-β-CD inclusion complexes, and physical mixtures are presented in Fig. 3. For the FT-IR spectra of GTE, the peak at 3228 cm^{-1} was associated to the O–H groups stretching vibration assigned to –OH group of polyphenols specially catechins (Rolim et al., 2019). Peaks at 2917 cm^{-1} and 2849 cm^{-1} were related to the C–H and $–CH_2–$ stretching vibration related to aliphatic hydrocarbons. Peak at 1692 cm^{-1} was assigned to C═C stretching of aromatic ring, and C═O stretching of conjugated carboxylic acids, quinones, ketones and esters (Sun et al., 2014). Peaks at 1608 cm^{-1} and 1448 cm^{-1} were assigned to C═C stretching vibration of aromatic ring of flavonoids. The peak at 1340 cm^{-1} was assigned to C–N vibration stretching of aromatic amines, representing the existence of water-soluble caffeine. The peak at 1232 cm^{-1} was assigned to C═O stretching due to conjugation of the oxygen. Peak at 1196 cm^{-1} and 1028 cm^{-1} were assigned to the carbonyl group and C–O–C stretching vibration, respectively.

As shown in Fig. 3, the β-CD displayed typical peaks at 3274 cm^{-1} for O–H group stretching vibration, at 2917 cm^{-1} for C–H and CH_2 stretching vibrations (Wang, Luo, & Xiao, 2014), at 1643 cm^{-1} for H–O–H bending of water molecules adhered to β-CD, at 1413 cm^{-1} for C–C–H and O–C–H bending, at 1151 cm^{-1} for C–O–C asymmetric stretching vibration, and at 1019 cm^{-1} for C–O–C symmetric stretching vibration (Abarca, Rodríguez, Guarda, Galotto, & Bruna, 2016). Peaks at 1030 and 1080 cm^{-1} for C–C stretching vibrations, at 938 cm^{-1} for skeletal vibration concerning the α1,4 linkage, at 857 cm^{-1} for C–C–H bending, C–O and C–C stretching of β-CD molecule were also observed.

In the case of physical mixture, the FT-IR spectrum showed some typical peaks attributable to individual patterns of GTE and β-CD, while minor variations in intensity were detected. These results specify that the physical mixture is not enough to encourage inclusion due to the absence of interactions between GTE and β-CD. As shown in Fig. 3, in the spectrum of the GTE-β-CD inclusion complex, GTE peaks were absolutely masked by very intense and broad β-CD peaks. In addition, the covering of guest molecule peaks by host molecule's broad and intense peaks could not affect the complex formation (Fang & Bhandari, 2010). Furthermore, upon complexation, peaks at 1643 cm^{-1}, 1413 cm^{-1}, and 1368 cm^{-1} shifted and showed reduction in intensity, whereas peaks at 2854 cm^{-1}, 1056 cm^{-1} and 992 cm^{-1} completely disappeared. These results specify that the occurrence of strong interactions between host and guest molecules obstructed some vibration mode (Xu, Zhang, Li, & Zheng, 2017). In addition, the peak intensity at 1024 cm^{-1} of inclusion complex was significantly improved, suggesting that bend vibration of O–H groups in the β-CD was enhanced. However, the peak at 3296 cm^{-1} of inclusion complex shown lower intensity than β-CD alone. This might indicate that O–H groups of flavonoids were embedded into β-CD cavities.

3.4. Thermal properties

TGA analysis was used to assess thermal stabilities of materials by their mass changes as a function of temperature. Its use is crucial for the authentication of complex formation. TGA thermograms and derivatives (DTG) for raw materials, their GTE-β-CD inclusion complexes, and physical mixtures are illustrated in Fig. 4. In general, the presence of peak in the DTG thermogram represents the temperature of highest rate for weight loss. From the results of TGA profiles, two regions with apparent weight loss were detected in the TGA profile of GTE (Fig. 4a). The first region of weight loss occurred at about 100 °C with 2.4% weight loss, which corresponded to evaporation of adsorbed water, solvent, or some extract volatiles (Rolim et al., 2019). The second region of weight loss happened at around 130 °C with 10–14% weight loss, which was assigned to thermal decomposition of polyphenols of the GTE. Besides, the weight loss (around 8–10%) of GTE continued up to 900 °C. This might be due to the decomposition of resistant aromatic structures of GTE (Sun et al., 2014).

TGA thermogram of β-CD (Fig. 4b) showed three distinct regions with possible weight loss. The first region happened at around 100 °C with 13.31% weight loss. It was ascribed to the evaporation of the superficial water molecules adsorbed by β-CD as well as the loss of water molecules positioned in the β-CD cavity (Abarca et al., 2016). The second region happened around 305 °C, corresponding to the main degradation process. In addition, at this stage, most of β-CD structures were decomposed with 75.83% weight loss. Finally, a third region occurred around 350 °C. It could be associated to the decomposition of carbonaceous matters in solid particles at a very slow rate.

As shown in Fig. 4e–f, TGA profile of GTE-β-CD revealed a loss of the melting peak of GTE and a dropping of β-CD dehydration signals as signs of complexation. However, TGA profile of GTE-β-CD displayed three regions where GTE-β-CD weight loss happened. The first region happened at around 100 °C with 14.05% weight loss, corresponding to disappearance of water moieties associated with the β-CD structure. The second region happened at around 265 °C with 64.21% weight loss.

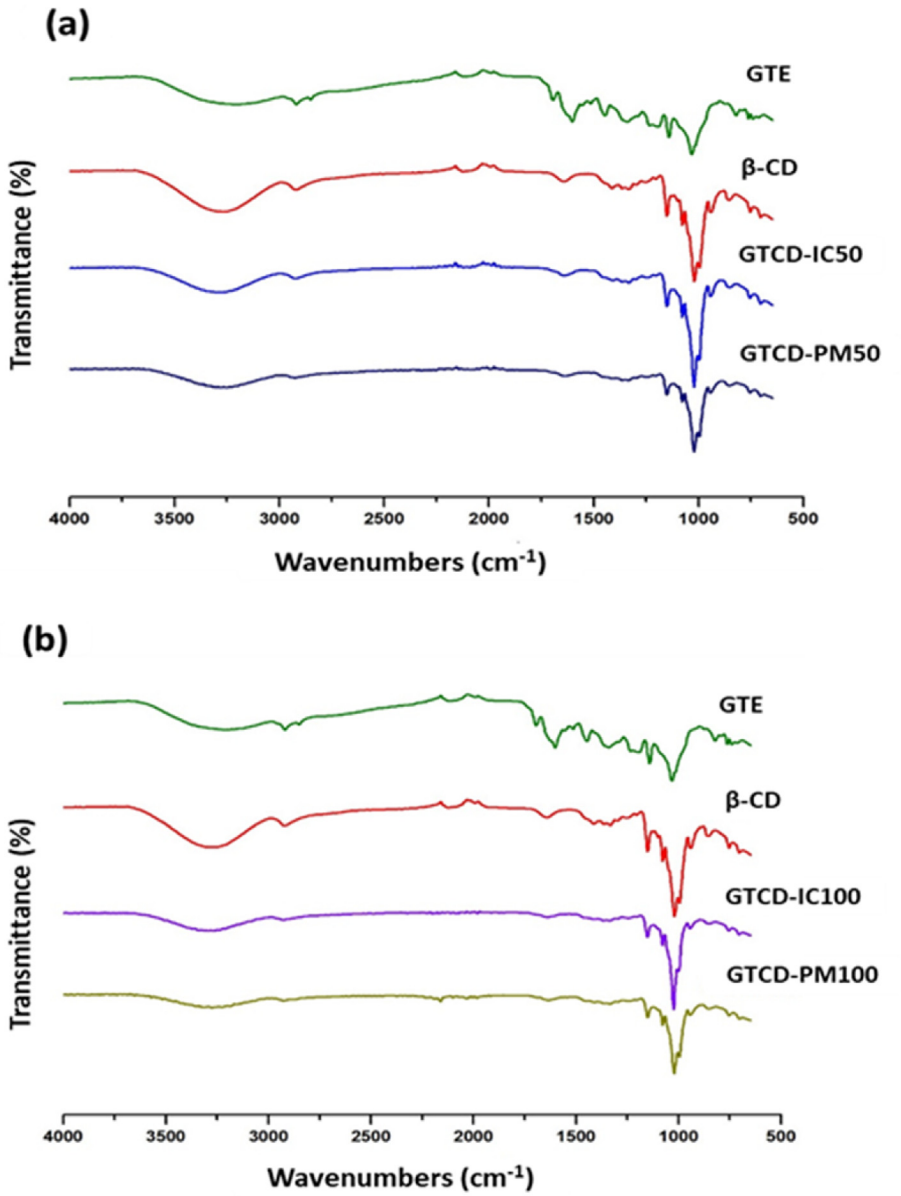

Fig. 3. FT-IR spectra of ethanolic extract of green tea (GTE), β-cyclodextrin (β-CD), physical mixtures (GTCD-PM50 and GTCD-PM100), and inclusion complexes (GTCD-IC50 and GTCD-IC100). (For interpretation of the references to colour in this figure legend, the reader is referred to the Web version of this article.)

It could be attributed to the decomposition of inclusion complexes. These consequences showed that complexation might expand the thermal stability of guest compounds. Several studies have informed that hos-guest interactions can significantly heighten the thermal stability of guest molecules embedded in the β-CD cavity (Fang & Bhandari, 2010; Jaski et al., 2019). Finally, the third region happened at around 355 °C. It might be related to the decomposition of carbonaceous matters in solid particles at a very slow rate. To confirm the complex formation, TGA was performed for physical mixtures of β-CD and GTE (Fig. 4c–d). These physical mixtures showed three distinct regions with weight loss (around 100 °C, 280 °C and 360 °C, respectively). These stages, with increasing temperature, generated analogous thermograms to those of raw materials, representing that water molecule, GTE, and β-CD were major components of this physical mixture (Devasari et al., 2015). In addition, decreased thermal stability of β-CD in the inclusion complex confirmed that complex formation was achieved.

3.5. Metabolite profiling of GTE-β-CD inclusion complexes

To elucidate differences in metabolites of GTE among the GTE-β-CD inclusion complexes and physical mixtures, we performed comprehensive metabolite profiling using UHPLC-LTQ-Orbitrap-MS combined with multivariate analysis including an unsupervised PCA model and a supervised PLS-DA model. PCA and PLS-DA score plots of samples analyzed by UHPLC-LTQ-Orbitrap-MS are shown in Fig. 5. In the PCA score plot, each group of physical mixtures (GTCD-PM50 and GTCD-PM100), and GTE-β-CD inclusion complexes (GTCD-IC50 and GTCD-IC100) presented clear grouping in each complexation procedure. As shown in PCA score plot (Fig. 5a), depending on the concentration of GTE used to make physical mixtures and inclusion complexes clearly separated by PC1 (27.1%). In addition, GTCD-IC50 and GTCD-IC100 were separated along with PC2 (16.6%). The PLS-DA score plot showed identical distribution patterns compared to PCA score plot. Statistical parameters of PLS-DA models were evaluated, showing R^2X of 0.606, R^2Y of 0.995, Q^2 of 0.780, and cross-validation p-value ($p < 0.05$) indicating the prediction accuracy, fitness, and the quality of the model

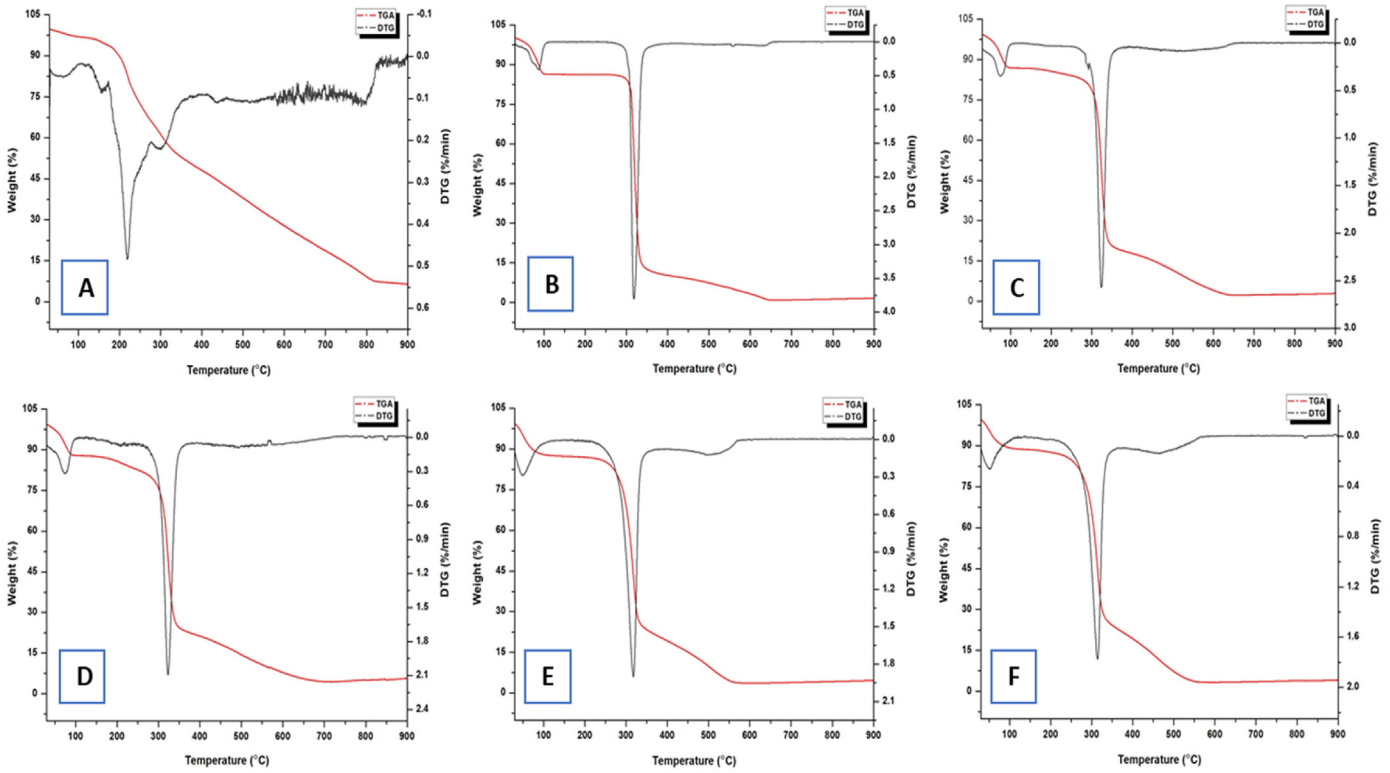

Fig. 4. TGA/DTG thermograms of ethanolic extract of green tea (**a**), β-cyclodextrin (**b**), physical mixtures (**c** and **d**), and inclusion complexes (**e** and **f**). (For interpretation of the references to colour in this figure legend, the reader is referred to the Web version of this article.)

as shown in Fig. 5b.

Metabolites significantly contributing to distributions of experimental groups in PLS-DA model were selected based on VIP value (> 0.7) derived from UHPLC-LTQ-Orbitrap-MS dataset. Among them, 20 metabolites (8 catechins, 1 polyol, 11 flavonols) were annotated and they showed statistically significant different quantities among the physical mixtures and GTE-β-CD inclusion complexes. Table 1 shows the detailed information about metabolites of GTE among the GTE-β-CD inclusion complexes and physical mixtures. Selective inclusion characteristics of β-CD were represented by comparing the changes in the content of each identified compound using UHPLC-LTQ-Orbitrap-MS (Fig. 6), and heat maps demonstrated their fold changes were illustrated in Fig. 7. In general, the variations in the relative contents of metabolites of the plant extracts in inclusion complexes might be possible due to the differences in processing methods, agitation time, and the ratio of host and guest materials (Fang & Bhandari, 2010). As can be seen from Table 1 and Fig. 7, among the tested samples, the content of all metabolites were similar, indicating that a variety of GTE

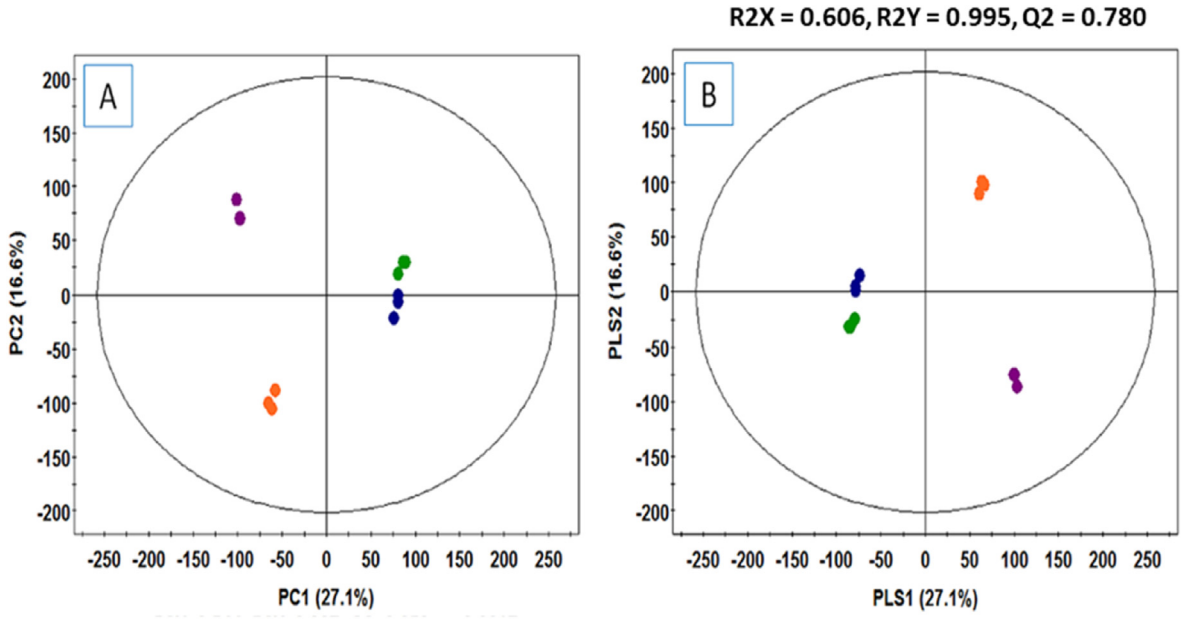

Fig. 5. PCA score plot and PLS-DA score plot of physical mixtures, and inclusion complexes (● GTCD-PM50, ● GTCD-PM100, ● GTCD-IC50, ● GTCD-IC100). PCA score plot (**a**) and PLS-DA score plot (**b**) derived from UHPLC-LTQ-Orbitrap-MS analysis.

Table 1
Discriminated metabolites of physical mixtures, and GTE-β-CD inclusion complexes analyzed by UHPLC-LTQ-Orbitrap-MS.

No.	Tentative identification[a]	Ret. (min)[b]	M.W.[b]	$[M-H]^-$	MS/MS fragments (m/z)	Molecular formula	**mDa (Δppm)**
1	Epigallocatechin (EGC)	3.11	306	305.0641	179/221/219/261	$C_{15}H_{14}O_7$	2.30
2	Epicatechin (EC)	4.07	290	289.0694	245/205/179/271	$C_{15}H_{14}O_6$	2.58
3	Epigallocatechin gallate (EGCG)	4.20	458	457.0733	169/331/305/287	$C_{22}H_{18}O_{11}$	0.86
4	Epicatechin gallate (ECG)	4.74	442	441.0789	289/169/331/271	$C_{22}H_{18}O_{10}$	1.47
5	Procyanidin	3.87	578	577.1307	425/407/451/289	$C_{30}H_{26}O_{12}$	2.13
6	3-Galloylprocyanidin b1	4.40	730	729.1404	407/559/577/451	$C_{37}H_{30}O_{16}$	3.28
7	Epiafzelechin 3-gallate	5.11	426	425.0848	273/169/255/381	$C_{22}H_{18}O_9$	−1.03
8	Epigallocatechin 3-p-coumaroate	5.26	452	451.0997	305/287/269/325	$C_{24}H_{20}O_9$	−0.81
9	3-O-p-Coumaroylquinic acid	4.14	338	337.0902	173/163/191/292	$C_{16}H_{18}O_8$	2.37
10	Myricetin galactoside-gallate	4.33	632	631.0885	479/563/316/317	$C_{28}H_{24}O_{17}$	2.69
11	Apigenin 6-C-glucoside 8-C-arabinoside	4.33	564	563.1353	473/443/353/383	$C_{26}H_{28}O_{14}$	1.51
12	Myricetin 3-*O*-rutinoside	4.40	626	625.1359	316/607/271/463	$C_{27}H_{30}O_{17}$	3.47
13	Myricetin 3-*O*-galactoside or Myricetin 3-O-glucoside	4.46	480	479.0790	316/317/309/269	$C_{21}H_{20}O_{13}$	3.35
14	Quercetin 3-O-glucosyl-rutinoside	4.52	772	771.1916	301/609/343/271	$C_{33}H_{40}O_{21}$	2.03
15	Apigenin 6-C-arabinosyl-8-C-xyloside	4.59	534	533.1256	443/473/383/515	$C_{25}H_{26}O_{13}$	2.63
16	Kaempferol 3-O-galactosylrutinoside	4.64	756	755.1980	285/593/257/301	$C_{33}H_{40}O_{20}$	−0.37
17	Quercetin 3-*O*-rutinoside	4.65	610	609.1410	301/457/343/271	$C_{27}H_{30}O_{16}$	3.83
18	Apigenin O-glucoside	4.68	432	431.0954	311/341/413/283	$C_{21}H_{20}O_{10}$	2.59
19	Kaempferol 3-O-rutinoside	4.88	594	593.1465	285/327/257/547	$C_{27}H_{30}O_{15}$	−0.23
20	Kaempferol 3-*O*-glucoside	5.01	448	447.0896	284/285/327/255	$C_{21}H_{20}O_{11}$	−0.13

[a] Tentative metabolites based on VIP > 0.7 and $p < 0.05$.
[b] RT and MW indicates rendition time and molecular weight, respectively.

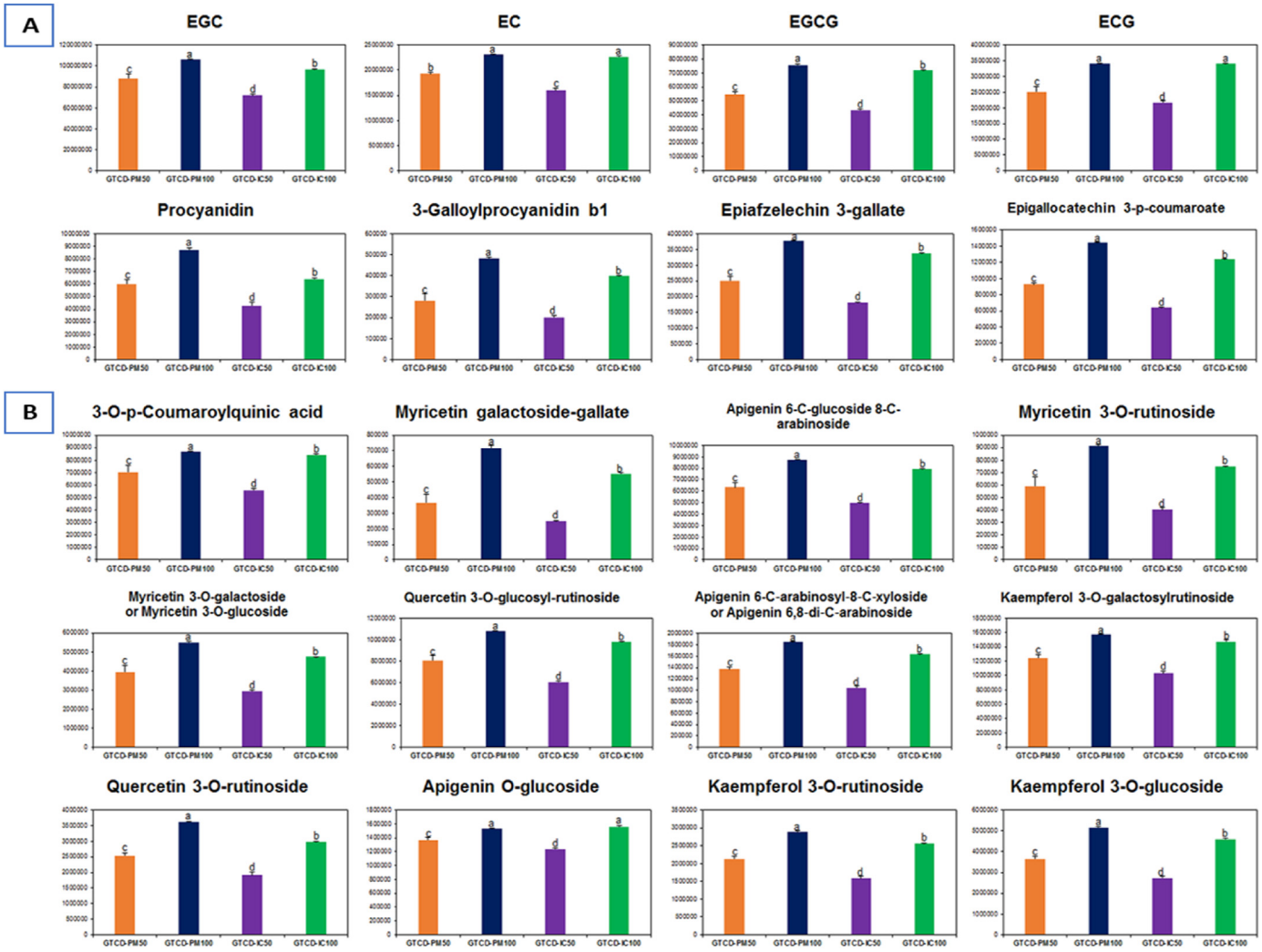

Fig. 6. The graph of metabolites showing significantly different contents among experimental groups. **(a)** Catechins, **(b)** Polyol and flavonols. Symbols including EGC, EC, EGCG, and ECG indicates epigallocatechin, epicatechin, epigallocatechin gallate, and epicatechin gallate, respectively.

No.	Tentative identification	Type of samples			
		GTCD-PM50	GTCD-PM100	GTCD-IC50	GTCD-IC100
1	Epigallocatechin (EGC)	0.97	1.17	0.79	1.06
2	Epicatechin (EC)	0.95	1.14	0.79	1.12
3	Epigallocatechin gallate (EGCG)	0.89	1.23	0.71	1.17
4	Epicatechin gallate (ECG)	0.88	1.19	0.75	1.18
5	Procyanidin	0.95	1.37	0.67	1.01
6	3-Galloylprocyanidin b1	0.82	1.42	0.59	1.17
7	Epiafzelechin 3-gallate	0.88	1.32	0.63	1.18
8	Epigallocatechin 3-*p*-coumaroate	0.87	1.36	0.60	1.16
9	3-*O*-*p*-Coumaroylquinic acid	0.94	1.17	0.75	1.13
10	Myricetin galactoside-gallate	0.78	1.52	0.53	1.17
11	Apigenin 6-*C*-glucoside 8-*C*-arabinoside	0.93	1.25	0.71	1.11
12	Myricetin 3-*O*-rutinoside	0.89	1.38	0.61	1.13
13	Myricetin 3-*O*-galactoside or Myricetin 3-*O*-glucoside	0.92	1.28	0.69	1.11
14	Quercetin 3-*O*-glucosyl-rutinoside	0.93	1.25	0.70	1.13
15	Apigenin 6-*C*-arabinosyl-8-*C*-xyloside	0.93	1.25	0.71	1.11
16	Kaempferol 3-*O*-galactosylrutinoside	0.94	1.18	0.78	1.11
17	Quercetin 3-*O*-rutinoside	0.92	1.31	0.69	1.08
18	Apigenin *O*-glucoside	0.96	1.07	0.87	1.10
19	Kaempferol 3-*O*-rutinoside	0.93	1.26	0.69	1.12
20	Kaempferol 3-*O*-glucoside	0.90	1.28	0.68	1.14

Fig. 7. Heat map representation for the relative contents of significantly discriminant metabolites among experimental groups. Metabolites were selected by variable importance in the projection (VIP) value > 0.7, p-value < 0.05.

metabolites remained stable even after forming an inclusion complexes between GTE and β-CD. However, results shown that considering the concentration of physical mixture (GTCD-PM50), around 70–80% of GTE metabolites particularly catechins and flavonols were keenly involved in the inclusion complexation with β-CD. In case of GTCD-IC100, which used twice higher concentration of GTE than GTCD-IC50, they had 1.2–1.95-fold higher concentration of GTE than GTCD-IC50 (Fig. 7). These results shown that the different metabolites of GTE have different equilibria in solution that drive them to form inclusion complexes with β-CD. Commonly, less polar bioactive active compounds were more susceptible to inclusion into β-CD hydrophobic cavity. Further, the selective inclusion capacity to bioactive compounds of GTE in β-CD might be controlled based on their host-guest interactions, and the ratio of host and guest molecules (Fang & Bhandari, 2010). In general, the selective inclusion attributes of GTE in β-CD were affected by various factors, such as structure of the host and guest molecules, functional groups in the guest molecules, cyclodextrin cavity size, and interactions between host and guest molecules (Zhang et al., 2017). Also, the selective inclusion attributes of GTE in β-CD might be possible due to the existence of synergistic or antagonistic co-encapsulation among guest molecules (Del Valle, 2004).

3.6. Antioxidant activities of GTE-β-CD inclusion complexes

Results of different assays (DPPH, ABTS, and FRAP) to determine antioxidant activities of physical mixtures and GTE-β-CD inclusion complexes are presented in Fig. 8a–c. Previous studies have reported that bioactive compounds responsible for the antioxidant activity of GTE are catechins (Zaveri, 2006). Additionally, the GTE had significantly high quantities of catechins and its derivatives. Subsequently, the pure GTE showed incredible antioxidant capacity based on DPPH, ABTS, and FRAP assays, with values of 0.99 mM, 0.96 mM, and 0.97 mM TEAC, respectively. As shown in Fig. 8a–c, results of DPPH, ABTS, and FRAP were very similar. Antioxidant activities of physical mixtures and inclusion complexes had the following order: GTCD-PM100 > GTCD-IC100 > GTCD-PM50 > GTCD-IC50. Results showed that the scavenging effect of encapsulated GTE on free radicals might be purely dependent on the concentration of GTE solution. Moreover, these results displayed a similar trend to contents of metabolites present in physical mixtures and GTE-β-CD inclusion complexes (Table 1 and Fig. 7). In all assays, physical mixtures and inclusion complexes showed distinct antioxidant activities ($p < 0.05$), indicating that each sample contained a different quantity of active components. The flavonoid rich fraction of ethanolic extracts is the main contributor to the total extract's antioxidant and radical scavenging activities (Silva, Ferreres, Malva, & Dias, 2005). Also, the difference in antioxidant capacity specifies that complex formation is distinct between complexation procedures due to differences in processing methods such as water amount, agitation time, and method.

4. Conclusions

In this study, we prepared the inclusion complexes of catechins-rich green tea extract with β-cyclodextrin by freeze-drying method. Structural characteristics of GTE-β-CD inclusion complexes were examined by microscopic, spectral, thermal, and XRD analyses. Results showed that bioactive components of GTE were effectively included in the cavity of β-CD to form the inclusion complex. After inclusion complexation, the samples were examined by UHPLC-LTQ-Orbitrap-MS and the variation in the quantities of each identified metabolite were visualized in the heat map. UHPLC-LTQ-Orbitrap-MS data confirmed a broad image of complexation results and shown a selective inclusion capacity to bioactive compounds particularly catechins and flavonols of green tea in β-CD based on their host-guest interaction. TGA results

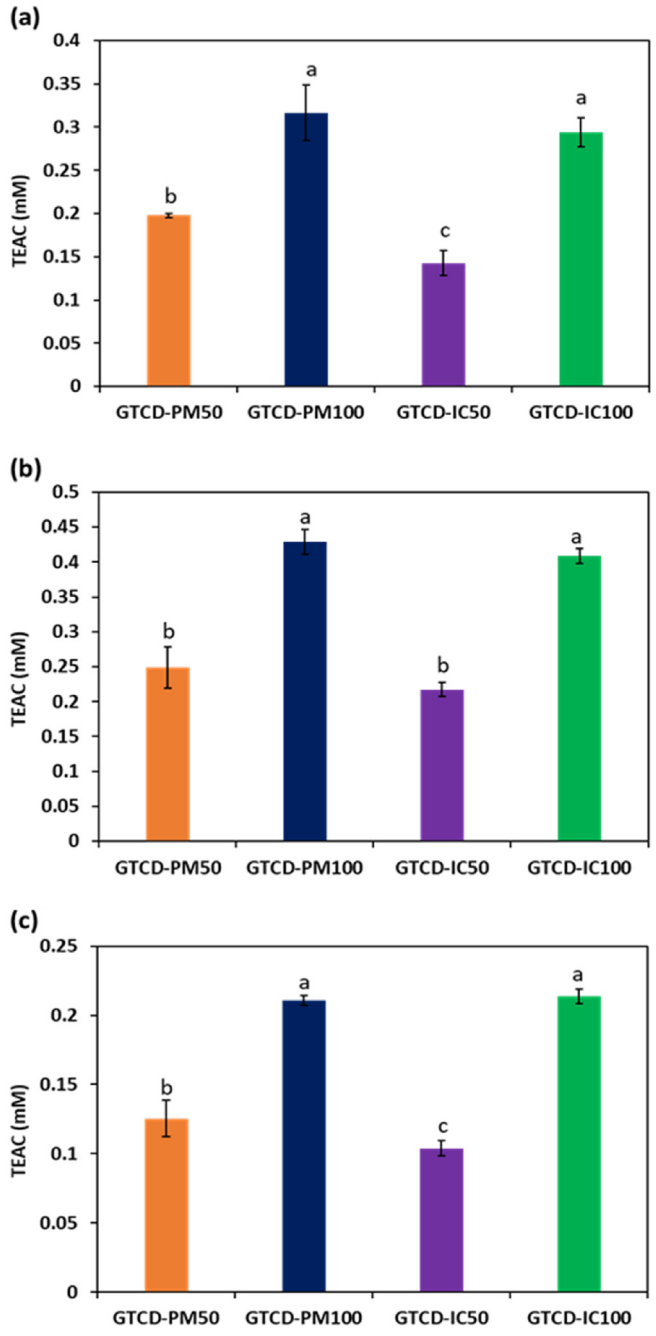

Fig. 8. Antioxidant activity assays of physical mixtures, and inclusion complexes. **(a)** DPPH, **(b)** ABTS, **(c)** FRAP.

confirmed that the thermal stability of GTE was upgraded significantly by complexation with β-CD. GTE-β-CD inclusion complexes showed higher scavenging capacities against DPPH and $ABTS^{+}$ radicals. These findings suggest that the GTE-β-CD inclusion complexes can enhance the thermal stability and bioavailability activities of GTE. This may increase applications of GTE in food and non-food industries.

CRediT authorship contribution statement

Chagam Koteswara Reddy: Conceptualization, Methodology, Data curation, Validation, Software, Writing - original draft. **Eun Sung Jung:** Data curation, Validation, Software, Writing - review & editing. **Su Young Son:** Data curation, Validation, Software. **Choong Hwan Lee:** Conceptualization, Project administration, Supervision, Resources, Writing - review & editing.

Declaration of competing interest

Authors have no conflict of interest to disclose.

Acknowledgements

This work was supported by Konkuk University (2017), Republic of Korea.

References

Abarca, R. L., Rodríguez, F. J., Guarda, A., Galotto, M. J., & Bruna, J. E. (2016). Characterization of beta-cyclodextrin inclusion complexes containing an essential oil component. *Food Chemistry, 196*, 968–975.

Aree, T., & Jongrungruangchok, S. (2016). Crystallographic evidence for β-cyclodextrin inclusion complexation facilitating the improvement of antioxidant activity of tea (+)-catechin and (−)-epicatechin. *Carbohydrate Polymers, 140*, 362–373.

Bancirova, M. (2010). Comparison of the antioxidant capacity and the antimicrobial activity of black and green tea. *Food Research International, 43*(5), 1379–1382.

Cai, R., Yuan, Y., Cui, L., Wang, Z., & Yue, T. (2018). Cyclodextrin-assisted extraction of phenolic compounds: Current research and future prospects. *Trends in Food Science & Technology, 79*, 19–27.

Chen, X., Chen, R., Guo, Z., Li, C., & Li, P. (2007). The preparation and stability of the inclusion complex of astaxanthin with β-cyclodextrin. *Food Chemistry, 101*(4), 1580–1584.

Del Valle, E. M. (2004). Cyclodextrins and their uses: A review. *Process Biochemistry, 39*(9), 1033–1046.

Devasari, N., Dora, C. P., Singh, C., Paidi, S. R., Kumar, V., Sobhia, M. E., et al. (2015). Inclusion complex of erlotinib with sulfobutyl ether-β-cyclodextrin: Preparation, characterization, in silico, in vitro and in vivo evaluation. *Carbohydrate Polymers, 134*, 547–556.

Fang, Z., & Bhandari, B. (2010). Encapsulation of polyphenols–a review. *Trends in Food Science & Technology, 21*(10), 510–523.

Han, X., Zhang, Z., Shen, H., Zheng, J., & Zhang, G. (2019). Comparison of structures, physicochemical properties and in vitro bioactivity between ferulic acid-β-cyclodextrin conjugate and the corresponding inclusion complex. *Food Research International, 125* 108619.

Ho, S., Thoo, Y. Y., Young, D. J., & Siow, L. F. (2017). Inclusion complexation of catechin by β-cyclodextrins: Characterization and storage stability. *Lebensmittel-Wissenschaft & Technologie, 86*, 555–565.

Hsu, C.-M., Yu, S.-C., Tsai, F.-J., & Tsai, Y. (2013). Enhancement of rhubarb extract solubility and bioactivity by 2-hydroxypropyl-β-cyclodextrin. *Carbohydrate Polymers, 98*(2), 1422–1429.

Jaski, J. M., Barão, C. E., Morais Lião, L., Silva Pinto, V., Zanoelo, E. F., & Cardozo-Filho, L. (2019). β-Cyclodextrin complexation of extracts of olive leaves obtained by pressurized liquid extraction. *Industrial Crops and Products, 129*, 662–672.

Jung, E. S., Park, H. M., Hyun, S. M., Shon, J. C., Lakshmanan, M., Noh, M., et al. (2017). Integrative metabolomic analysis reveals diet supplementation with green tea alleviates UVB-damaged mouse skin correlated with ascorbate metabolism and urea cycle. *Metabolomics, 13*(7), 82.

Kao, Y.-h., Hiipakka, R. A., & Liao, S. (2000). Modulation of obesity by a green tea catechin. *American Journal of Clinical Nutrition, 72*(5), 1232–1233.

Kim, H. R., Rajaiah, R., Wu, Q.-L., Satpute, S. R., Tan, M. T., Simon, J. E., et al. (2008). Green tea protects rats against autoimmune arthritis by modulating disease-related immune events. *Journal of Nutrition, 138*(11), 2111–2116.

Krishnaswamy, K., Orsat, V., & Thangavel, K. (2012). Synthesis and characterization of nano-encapsulated catechin by molecular inclusion with beta-cyclodextrin. *Journal of Food Engineering, 111*(2), 255–264.

Liu, M., Zheng, Y., Wang, C., Xie, J., Wang, B., Wang, Z., et al. (2016). Improved stability of (+)-catechin and (−)-epicatechin by complexing with hydroxypropyl-β-cyclodextrin: Effect of pH, temperature and configuration. *Food Chemistry, 196*, 148–154.

Lorenzo, J. M., & Munekata, P. E. S. (2016). Phenolic compounds of green tea: Health benefits and technological application in food. *Asian Pacific Journal of Tropical Biomedicine, 6*(8), 709–719.

Lu, T.-M., Lee, C.-C., Mau, J.-L., & Lin, S.-D. (2010). Quality and antioxidant property of green tea sponge cake. *Food Chemistry, 119*(3), 1090–1095.

Okumura, H., Kawaguchi, Y., & Harada, A. (2003). Preparation and characterization of the inclusion complexes of poly (dimethylsilane) s with cyclodextrins. *Macromolecules, 36*(17), 6422–6429.

Pu, H., Sun, Q., Tang, P., Zhao, L., Li, Q., Liu, Y., et al. (2018). Characterization and antioxidant activity of the complexes of tertiary butylhydroquinone with β-cyclodextrin and its derivatives. *Food Chemistry, 260*, 183–192.

Rolim, W. R., Pelegrino, M. T., de Araújo Lima, B., Ferraz, L. S., Costa, F. N., Bernardes, J. S., et al. (2019). Green tea extract mediated biogenic synthesis of silver nanoparticles: Characterization, cytotoxicity evaluation and antibacterial activity. *Applied Surface Science, 463*, 66–74.

Silva, B. A., Ferreres, F., Malva, J. O., & Dias, A. C. P. (2005). Phytochemical and antioxidant characterization of Hypericum perforatum alcoholic extracts. *Food Chemistry, 90*(1), 157–167.

Sun, Q., Cai, X., Li, J., Zheng, M., Chen, Z., & Yu, C.-P. (2014). Green synthesis of silver nanoparticles using tea leaf extract and evaluation of their stability and antibacterial activity. *Colloids and Surfaces A: Physicochemical and Engineering Aspects, 444*, 226–231.

Wang, J., Cao, Y., Sun, B., & Wang, C. (2011). Physicochemical and release characterisation of garlic oil-β-cyclodextrin inclusion complexes. *Food Chemistry, 127*(4), 1680–1685.

Wang, X., Luo, Z., & Xiao, Z. (2014). Preparation, characterization, and thermal stability of β-cyclodextrin/soybean lecithin inclusion complex. *Carbohydrate Polymers, 101*, 1027–1032.

Wen, P., Zhu, D.-H., Wu, H., Zong, M.-H., Jing, Y.-R., & Han, S.-Y. (2016). Encapsulation of cinnamon essential oil in electrospun nanofibrous film for active food packaging. *Food Control, 59*, 366–376.

Xu, J., Zhang, Y., Li, X., & Zheng, Y. (2017). Inclusion complex of nateglinide with sulfobutyl ether β-cyclodextrin: Preparation, characterization and water solubility. *Journal of Molecular Structure, 1141*, 328–334.

Ye, X., Chen, Z., Zhang, Y., Mu, J., Chen, L., Li, B., et al. (2020). Construction, characterization, and bioactive evaluation of nano-selenium stabilized by green tea nano-aggregates. *Lebensmittel-Wissenschaft & Technologie, 129* 109475.

Zaveri, N. T. (2006). Green tea and its polyphenolic catechins: Medicinal uses in cancer and noncancer applications. *Life Sciences, 78*(18), 2073–2080.

Zhang, S., Zhang, H., Xu, Z., Wu, M., Xia, W., & Zhang, W. (2017). Chimonanthus praecox extract/cyclodextrin inclusion complexes: Selective inclusion, enhancement of antioxidant activity and thermal stability. *Industrial Crops and Products, 95*, 60–65.